



UNIVERSITY OF LEEDS

This is a repository copy of *Haldane-Hubbard Mott Insulator: From Tetrahedral Spin Crystal to Chiral Spin Liquid*.

White Rose Research Online URL for this paper:  
<http://eprints.whiterose.ac.uk/93917/>

Version: Accepted Version

---

**Article:**

Hickey, C, Cincio, L, Papić, Z et al. (1 more author) (2016) Haldane-Hubbard Mott Insulator: From Tetrahedral Spin Crystal to Chiral Spin Liquid. *Physical Review Letters*, 116 (13). 137202. ISSN 0031-9007

<https://doi.org/10.1103/PhysRevLett.116.137202>

---

**Reuse**

Unless indicated otherwise, fulltext items are protected by copyright with all rights reserved. The copyright exception in section 29 of the Copyright, Designs and Patents Act 1988 allows the making of a single copy solely for the purpose of non-commercial research or private study within the limits of fair dealing. The publisher or other rights-holder may allow further reproduction and re-use of this version - refer to the White Rose Research Online record for this item. Where records identify the publisher as the copyright holder, users can verify any specific terms of use on the publisher's website.

**Takedown**

If you consider content in White Rose Research Online to be in breach of UK law, please notify us by emailing [eprints@whiterose.ac.uk](mailto:eprints@whiterose.ac.uk) including the URL of the record and the reason for the withdrawal request.



[eprints@whiterose.ac.uk](mailto:eprints@whiterose.ac.uk)  
<https://eprints.whiterose.ac.uk/>

# Haldane-Hubbard Mott Insulator: From Tetrahedral Spin Crystal to Chiral Spin Liquid

Ciarán Hickey,<sup>1</sup> Lukasz Cincio,<sup>2</sup> Zlatko Papić,<sup>3</sup> and Arun Paramekanti<sup>1,4</sup>

<sup>1</sup>*Department of Physics, University of Toronto, Toronto, Ontario M5S 1A7, Canada*

<sup>2</sup>*Perimeter Institute for Theoretical Physics, Waterloo, Ontario N2L 2Y5, Canada*

<sup>3</sup>*School of Physics and Astronomy, University of Leeds, Leeds, LS2 9JT, United Kingdom and*

<sup>4</sup>*Canadian Institute for Advanced Research, Toronto, Ontario M5G 1Z8, Canada*

Motivated by cold atom experiments on Chern insulators, we study the honeycomb lattice Haldane-Hubbard Mott insulator of spin-1/2 fermions using exact diagonalization and density matrix renormalization group methods. We show that this model exhibits various chiral magnetic orders including a wide regime of triple-Q tetrahedral order. Incorporating third-neighbor hopping frustrates and ultimately melts this tetrahedral spin crystal. From analyzing the low energy spectrum, many-body Chern numbers, entanglement spectra, and modular matrices, we identify the molten state as a chiral spin liquid (CSL) with gapped semion excitations. We formulate and study the Chern-Simons-Higgs field theory of the exotic CSL-to-tetrahedral spin crystallization transition.

Electronic bands in crystals can display nontrivial topology, as exemplified by the recent discoveries of topological insulators [1, 2], Weyl semimetals [3–5], and quantum anomalous Hall insulators (QAHI) [6, 7]. Interactions can dramatically modify this single-particle physics, for instance by rendering indistinguishable certain topologically distinct free-fermion phases [8, 9]. An alternative outcome is the emergence of topological order [10], manifested by nontrivial ground state degeneracies depending on the lattice topology, as discovered in numerical studies of partially filled Chern bands which realize lattice fractional quantum Hall liquids [11, 12]. Interactions may also lead to charge localization, while the spin degrees of freedom display topological order. Finding even quasi-realistic models of such topological Mott insulators (TMIs) [13–16] is a crucial step towards identifying experimental candidates and understanding exotic quantum phase transitions out of TMIs.

In this Letter, we study interaction effects in the Haldane model [17], a paradigmatic model of a QAHI on the two-dimensional (2D) honeycomb lattice. The Haldane model supports two bands with Chern numbers  $C = \pm 1$ ; it has been realized in recent cold atom experiments [18, 19]. We study the effect of strong Hubbard repulsion on spin-1/2 (i.e., two-component) fermions in the Haldane model, at a filling of one fermion per site, obtaining the following key results. (i) We establish that the effective spin model for the Haldane-Mott insulator exhibits a variety of chiral magnetic orders including a wide regime of tetrahedral order with large scalar spin chirality. Our results are obtained using exact diagonalization (ED) on cluster of up to  $N = 32$  spins. (ii) Incorporating third-neighbor hopping is shown to frustrate and ultimately melt the tetrahedral order. Our ED results in the liquid phase find a gapped, approximately two-fold degenerate ground state, with total many-body Chern number  $C = 1$ , suggesting that this state is a chiral spin liquid (CSL): the  $\nu = 1/2$  bosonic quantum Hall state with gapped semion excitations [20–22]. We provide conclusive evidence for this using state-of-the-art density matrix renormalization group (DMRG) [23, 24] computations on infinitely long cylinders with circumference up to 8 lattice unit cells, computing entanglement spectra, quantum dimensions of all anyon types, and quasiparticle braiding

properties via topological  $S$  and  $T$  matrices. This frustration-induced melting of tetrahedral order is a completely *distinct* mechanism to realize CSLs compared with previous studies, and allows us, for the first time, to identify the tetrahedral state as a ‘parent’ state for the CSL. (iii) Our ED results suggest a continuous phase transition between the tetrahedral state and the CSL. We formulate a Chern-Simons-Higgs field theory to describe this exotic spin crystallization transition out of the topologically ordered CSL.

The study of CSLs was rejuvenated by the construction of exact parent Hamiltonians [25, 26], and recent works have found evidence for CSLs on the kagome [27–36] and square lattices [37, 38], and in certain  $SU(N)$  Mott insulators [39] and coupled wire models [40, 41]. Our work provides the first example of a CSL on the honeycomb lattice in a realistic model starting from fermions with on-site interactions. This is nontrivial since a symmetric spin-gapped phase on lattices with even number of spin-1/2 per unit cell is not guaranteed to have topological order [42, 43]. Our work goes well beyond previous work on this model [44–48], and studies of Gutzwiller projected Chern-insulator wavefunctions [49, 50] which did not consider microscopic models that support such ground states. The tetrahedral state we find here also occurs in certain triangular lattice Hubbard and Kondo models [51, 52], suggesting that such frustration-induced CSLs may appear in a wider class of models and materials.

**Model.** The Haldane-Hubbard model for spin-1/2 fermions shown in Fig. 1(a) is defined by the Hamiltonian

$$H_{\text{HH}} = -t_1 \sum_{\langle ij \rangle \sigma} (c_{i\sigma}^\dagger c_{j\sigma} + h.c.) - t_2 \sum_{\langle\langle ij \rangle\rangle \sigma} (e^{i\nu_{ij}\phi} c_{i\sigma}^\dagger c_{j\sigma} + h.c.) + U \sum_i n_{i\uparrow} n_{i\downarrow}, \quad (1)$$

where  $\langle \cdot \rangle$  and  $\langle\langle \cdot \rangle\rangle$  denote, respectively, first and second nearest neighbors,  $\nu_{ij} = \pm 1$  produces a flux pattern with a net zero flux per unit cell, and  $U$  is the Hubbard repulsion. For  $U = 0$ , this model supports Chern bands for  $t_2, \phi \neq 0$ . At half-filling, this leads to a QAHI with  $\sigma_{xy} = \pm e^2/h$  per spin for small  $|t_2|$ . At large  $|t_2|$  and  $\phi \neq \pi/2$ , the Chern bands strongly disperse, leading to a metal with  $\sigma_{xy} \neq 0$  but non-quantized [47].

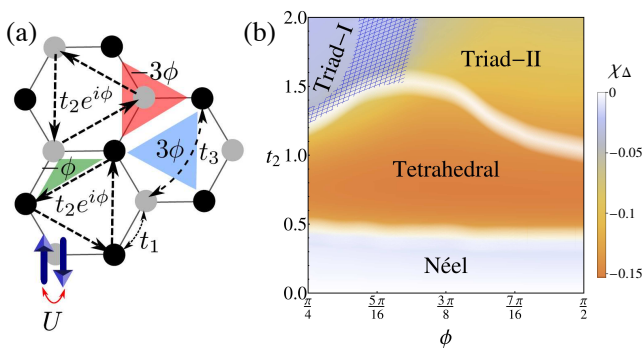


FIG. 1. (Color online) (a) Haldane-Hubbard model showing short distance hopping amplitudes, plaquette fluxes, and Hubbard repulsion  $U$ . (b) Phase diagram of  $H_{\text{spin}}$  for  $t_3 = 0$ ,  $U = 10$  from ED on clusters with  $N = 24$  spins; color indicates the chirality  $\langle \hat{\chi}_\Delta \rangle$  on small triangles. **Solid white lines indicate phase boundaries, broadened to account for finite-size effects.** In the hatched (blue) region we cannot sharply identify the phase in ED as Triad-I or II.

For  $U \gg |t_{1,2}|$ , degenerate perturbation theory in the Mott insulator [53] with one fermion per site leads to the spin model

$$H_{\text{spin}} = \frac{4t_1^2}{U} \sum_{\langle ij \rangle} \mathbf{S}_i \cdot \mathbf{S}_j + \frac{4t_2^2}{U} \sum_{\langle\langle ij \rangle\rangle} \mathbf{S}_i \cdot \mathbf{S}_j + \frac{24t_1^2 t_2}{U^2} \sum_{\text{small}-\Delta} \hat{\chi}_\Delta \sin \Phi_\Delta + \frac{24t_3^2}{U^2} \sum_{\text{big}-\Delta} \hat{\chi}_\Delta \sin \Phi_\Delta, \quad (2)$$

where  $\hat{\chi}_\Delta \equiv \mathbf{S}_i \cdot (\mathbf{S}_j \times \mathbf{S}_k)$  is the scalar spin chirality operator. The sites  $\{ijk\}$  in  $\hat{\chi}_\Delta$  are labelled going anticlockwise around the small or big triangles of the honeycomb lattice. As shown in Fig. 1(a), the fluxes in  $H_{\text{spin}}$  are  $\Phi_\Delta = -\phi$  on small (green) triangles, and  $\Phi_\Delta = -3\phi$  ( $+3\phi$ ) on large triangles which do (do not) enclose a lattice site. Classical magnetic ground states of this model, valid for  $S = \infty$ , have been studied in [47]; here, we resort to a numerical study for  $S = 1/2$ , retaining strong quantum fluctuations.

**ED phase diagram.** For  $\phi = 0$ ,  $H_{\text{spin}}$  reduces to the  $J_1$ - $J_2$  honeycomb lattice Heisenberg model, with  $J_{1,2} = 4t_{1,2}^2/U$ . Previous work indicates that  $J_2 \gtrsim 0.2J_1$  kills Néel order, leading to incommensurate spirals [54] for  $S = \infty$ , and competing valence bond crystals for  $S = 1/2$  [55–57]. Here, we study the unexplored regime  $\phi \neq 0$ , using Lanczos ED on clusters up to  $N = 32$  spins, varying  $t_2$  and  $\phi$  for fixed  $U/t_1 = 10$  which puts us in the Mott insulator [47]. We focus on flux values  $\pi/4 \leq \phi \leq \pi/2$ , which reveals commensurate phases with large scalar spin chirality; restricting ourselves to this window of flux avoids incommensurate spiral orders [47, 54] expected at small  $\phi$ , which have strong finite-size effects in ED. Below, we work in units where  $t_1 = 1$ .

As shown in Fig. 1(b), we find that the phase diagram contains four magnetically ordered phases — Néel, tetrahedral and triad-I/II orders — which are also observed in the classical phase diagram [47]. (i) The Néel order on the honeycomb lattice is translationally invariant, with ferromagnetic order on

each sublattice and a single structure factor peak at the  $\Gamma$  point of the hexagonal Brillouin zone. (ii) The tetrahedral order has an 8-site magnetic unit cell, with spins pointing toward the four corners of a tetrahedron and structure factor peaks at the three  $M$  points. It is a so-called “regular magnetic order”, respecting all lattice symmetries modulo global spin rotations. (iii)/(iv) Triad-I/II both have 6-site magnetic unit cells, with three spins on each sublattice forming a cone and structure factor peaks at the  $K$  and  $K'$  points. They can be thought of as umbrella states on each triangular sublattice, with their common axis being parallel in the triad-I case and anti-parallel in the triad-II. This yields a net ferromagnetic moment in triad-I and a net staggered moment in triad-II.

We identify these magnetic orders within ED, **on clusters with up to  $N = 32$  spins**, through a careful analysis of the low energy spectrum, extracting quantum numbers of the quasi-degenerate joint states, i.e., the ‘Anderson tower’, in each total spin sector, whose energies collapse onto the ground state as  $1/N$  leading to spontaneous symmetry breaking in the thermodynamic limit [58, 59] (see Supplemental Material [60]). The phase boundaries in Fig. 1(b) are determined [60] by dips in the ground state fidelity  $\langle \Psi_0(g) | \Psi_0(g + \delta g) \rangle$  which signal quantum phase transitions [61], where  $g$  is a tuning parameter (here,  $t_2$  or  $\phi$ ). We substantiate this by studying changes in the finite-size singlet ( $E_s$ ) and triplet ( $E_t$ ) gaps,  $\langle \hat{\chi}_\Delta \rangle$ , and reorganization of the low energy spectrum. Our results are in contrast to slave-rotor mean field theory of the Haldane Mott insulator [44, 45], in which the ground state is a CSL which simply inherits the band topology of the underlying QAH.

**Melting tetrahedral order.** The tetrahedral state is a “regular magnetic state” [62] which respects all lattice symmetries in its  $SU(2)$ -invariant correlations. Given its large scalar spin chirality, it is tempting to speculate that quantum disordering this state might lead to a CSL. We thus modify the Haldane model in order to frustrate the tetrahedral order. We notice that the tetrahedral state has spins on opposite vertices of the honeycomb hexagon aligned ferromagnetically. Thus incorporating third-neighbor hopping  $t_3$  will lead to an additional exchange interactions in  $H_{\text{spin}}$ , i.e., the Heisenberg exchange  $J_3 = 4t_3^2/U > 0$  which will inevitably frustrate tetrahedral order, as well as additional chiral interactions. Below, we present extensive results retaining only  $J_3 > 0$  since keeping all chiral terms induced by  $t_3$  significantly increases the computational complexity; we have explicitly checked that these additional terms induce very small quantitative differences in the ED spectra, and only slightly shift the phase boundaries in the phase diagram (see Supplemental Material [60]).

One key signature of a CSL is a nonzero spin gap and two-fold ground state degeneracy on the torus. We thus look for regimes where the lowest excited state is a spin-singlet whose energy gap becomes smaller with system size, while the triplet gap remains nonzero. Fig. 2(a) shows the ED phase diagram as we vary  $(t_2, t_3)$ , where we find a candidate CSL regime. Here, we have fixed  $\phi = \pi/3$ , at which the coefficient of  $\hat{\chi}_\Delta$  on the large- $\Delta$  vanishes, enormously simplifying the numerics.

Fig. 2(c) shows a representative ED spectrum on an  $N = 32$

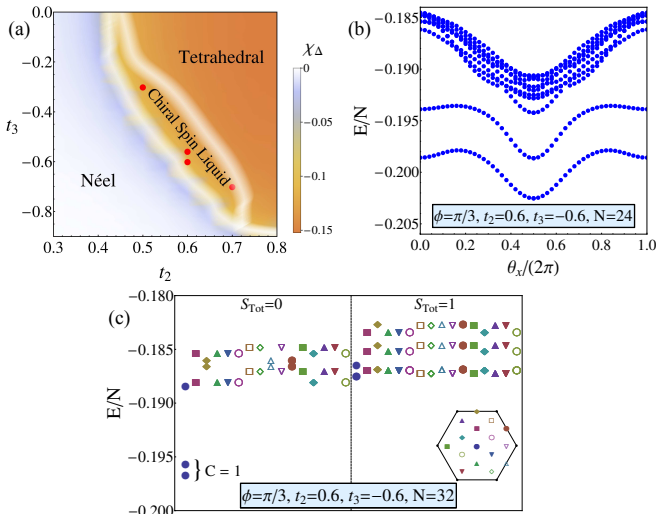


FIG. 2. (Color online) (a) Phase diagram of  $H_{\text{spin}}$  at  $\phi = \pi/3$  and  $U = 10$ , keeping the additional  $J_3$  term induced by  $t_3 \neq 0$ . Background shows ground state chirality  $\langle \hat{\chi}_\Delta \rangle$  on small- $\Delta$ . Using ED and DMRG (at indicated points), we find a window of CSL with topological order. (b) Topological robustness of the CSL ground states upon threading flux through one hole of the torus. Energy spectrum as a function of boundary phase  $\theta_x$  is shown for  $N = 24$  sites,  $t_2 = 0.6$ , and  $t_3 = -0.6$ . (c) Energy spectrum for  $N = 32$  cluster, with states labelled by total spin  $S_{\text{tot}}$  and Brillouin zone momenta shown in the inset. We find approximate two-fold ground state degeneracy with total Chern number  $C_1 + C_2 = 1$ .

torus at  $(t_2, t_3) = (0.6, -0.6)$ . We find an approximate two-fold ground state degeneracy, both states being spin singlets with crystal momentum  $\mathbf{k} = (0, 0)$  as expected for a honeycomb lattice CSL, and a spin gap  $E_t \approx 0.3$ . Threading flux through one hole of the torus (see Fig. 2(b)), we find the two-fold ground state manifold does not mix with higher excited states, demonstrating that the ground state degeneracy is of topological origin. We have computed the many-body Chern numbers  $C_i = -\frac{1}{\pi} \int d\theta_1 d\theta_2 \text{Im} \langle \partial_{\theta_1} \Psi_i | \partial_{\theta_2} \Psi_i \rangle$  using twisted boundary conditions on the two ground states  $|\Psi_{i=1,2}\rangle$ , since two ground states have the same momentum and thus do not cross. However, only the total Chern number of this degenerate manifold is meaningful in the thermodynamic limit; we find  $C_1 + C_2 = 1$ . These results provide strong evidence that  $t_3$  melts tetrahedral order, leading to a  $\nu = 1/2$  bosonic Laughlin liquid. Our ED results delineate a regime at  $\phi = \pi/3$ , see Fig. 2(a), which we identify as a CSL candidate. **DMRG results.** To further confirm the existence of CSL, we investigate the model  $H_{\text{spin}}$  with additional terms generated by non-zero  $t_3$ , using DMRG [24], on a cylinder of infinite length with circumference up to  $L = 8$  unit cells. The characterization of a topologically ordered phase is achieved by: (i) identifying the conformal field theory (CFT) that describes gapless edge excitations via the “entanglement spectrum” [63], and (ii) computing topological  $S$  and  $T$  matrices that contain information about bulk anyon excitations [22, 50, 64–67]. Simulations were performed for  $\phi = \pi/3$ ,

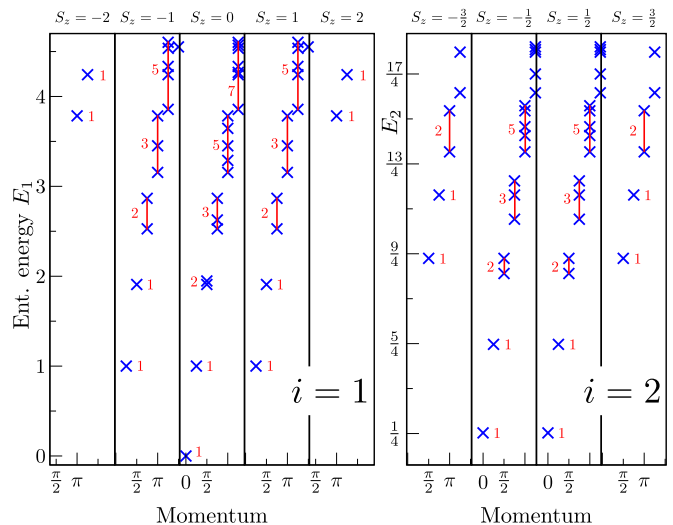


FIG. 3. (Color online) Entanglement spectrum (rescaled and shifted) of the reduced density matrix  $\rho_i$  for half an infinite cylinder (with circumference  $L = 8$  unit cells) computed for the ground states  $|\Psi_1^{\text{cy1}}\rangle$  (left panel) and  $|\Psi_2^{\text{cy1}}\rangle$  (right panel) of the effective spin model at  $(t_2, t_3, \phi) = (0.6, -0.6, \pi/3)$ . Vertical axes show entanglement energies defined as  $E_{i,\alpha} = -\log \lambda_{i,\alpha}$ , where  $\lambda_{i,\alpha}$  are the eigenvalues of  $\rho_i$ . The transverse momenta of the corresponding eigenvectors of  $\rho_i$  are shown on horizontal axes, separately for every tower labeled by  $S_z$  quantum number. The number of close lying states with the same momenta in a given  $S_z$  sector is shown in red.

and four different values of  $(t_2, t_3)$  marked by red dots on the phase diagram in Fig. 2(a), keeping only the additional  $J_3$  exchange term. We present detailed results below for one point  $(t_2, t_3) = (0.6, -0.6)$ ; we obtain similar results at the other three points. We also performed simulations on smaller width cylinders (upto  $L = 6$ ) keeping  $J_3$  and all additional chiral terms from having  $t_3 \neq 0$  in  $H_{\text{HH}}$ , obtaining similar results.

Randomly initialized DMRG finds two ground states,  $|\Psi_{i=1,2}^{\text{cy1}}\rangle$ , with well-defined anyon flux threading inside the cylinder [65]. Fig. 3 shows the entanglement spectrum  $E_i$  of the reduced density matrix for half an infinite cylinder computed for both ground states. Studying these spectra, we can extract universal information about possible gapless boundary excitations, as if the system had an actual, physical edge [63, 68–71]. The spectra  $E_i$  are seen to be consistent with corresponding sectors of the chiral  $SU(2)_1$  Wess-Zumino-Witten CFT [72].  $E_1$  is associated with the identity primary operator and its Kac-Moody descendants. The computed degeneracy pattern in every tower (labeled by  $S_z$ ) is seen to follow the expected partition numbers  $(1-1-2-3-5-7-\dots)$  [73].  $E_2$  corresponds to the chiral boson vertex operator and its descendants.

The ground states  $|\Psi_{i=1,2}^{\text{cy1}}\rangle$  on an infinite cylinder  $\infty \times L$  may be used to mimic ground states on a  $L \times L$  torus  $|\Psi_{i=1,2}^{\text{tor}}\rangle$  by means of cutting and reconnecting matrix-product states of  $|\Psi_i^{\text{cy1}}\rangle$  [65, 66]. Every such ground state  $|\Psi_i^{\text{tor}}\rangle$  has a well-defined anyon flux threading inside the torus. The topological  $S$  and  $T$  matrices of the emergent anyons can be extracted

[74] from the overlaps  $\langle \Psi_i^{\text{tor}} | R_{\pi/3} | \Psi_j^{\text{tor}} \rangle$ , where  $R_{\pi/3}$  denotes clockwise  $\pi/3$  rotation of a  $L \times L$  torus. For  $L = 6$ , we find

$$S = \frac{1}{\sqrt{2}} \begin{pmatrix} 0.99 & 0.97 \\ 0.96 & -0.97 \cdot e^{i\pi \cdot 0.01} \end{pmatrix}, \quad (3)$$

$$T = e^{i\frac{2\pi}{24} \cdot 0.96} \begin{pmatrix} 1 & 0 \\ 0 & -i \cdot e^{i\pi \cdot 0.01} \end{pmatrix}, \quad (4)$$

in excellent agreement with the exact  $S$  and  $T$  matrices of a chiral semion anyon model,  $\frac{1}{\sqrt{2}} \begin{pmatrix} 1 & 1 \\ 1 & -1 \end{pmatrix}$  and  $e^{i\frac{2\pi}{24}} \begin{pmatrix} 1 & 0 \\ 0 & -i \end{pmatrix}$ .

**The combined DMRG results thus provide an unambiguous identification of the phase as a CSL.**

**Spin crystallization transition.** Our ED results show that the chirality and ground state fidelity vary smoothly going from the tetrahedral state into the CSL. This suggests that the two phases might be separated by an exotic critical point since the tetrahedral state is topologically trivial but breaks  $SU(2)$  spin symmetry while the CSL has topological order and no broken symmetries. A powerful route to accessing such exotic transitions is via fractionalizing the spins [75]. We formulate our theory in terms of spin-1/2 bosonic spinons minimally coupled to an Abelian level  $k = 2$  Chern-Simons (CS) gauge field. In the CSL, integrating out gapped spinons results in a CS topological field theory. The lowest energy excitations are gapped spinons, which carry unit gauge charge and bind  $\pi$ -flux, converting them into semions. On the tetrahedral side, spinon condensation produces magnetic order, destroying topological order via the Higgs mechanism.

To construct the field theory for the matter sector, we imagine bosonic spinons with spins polarized along the local Zeeman axes of the underlying tetrahedral order. Adiabatic spinon transport around closed loops on the honeycomb lattice then produces nontrivial Berry phases; we find  $\pi$ -flux around hexagonal loops and  $\pi/2$ -flux around triangular plaquettes. Even if long wavelength quantum fluctuations disorder the tetrahedral state, so these Zeeman fields average to zero, we expect the local spin chirality and hence the local fluxes to persist. Diagonalizing this spinon Hofstadter Hamiltonian on the honeycomb lattice, we find 4 equivalent dispersion minima located, for our gauge choice, at  $\mathbf{Q}_0 \equiv \Gamma$  and  $\mathbf{Q}_i \equiv M_i$  ( $i = 1, 2, 3$ ; the three  $M$  points of the BZ). We thus study the action  $S = \int d^2x d\tau (\mathcal{L}_{\text{CS},\phi} + \mathcal{L}_{\text{int}})$ , where

$$\mathcal{L}_{\text{CS},\phi} = \frac{1}{2\pi} \epsilon^{\mu\nu\lambda} a_\mu \partial_\nu a_\lambda + \phi_{i\alpha}^* (\partial_\tau - ia_0) \phi_{i\alpha} + r |\phi_{i\alpha}|^2 + |(\vec{\nabla} - i\vec{a}) \phi_{i\alpha}|^2 \quad (5)$$

describes bosonic spinons minimally coupled to the CS gauge field, while  $\mathcal{L}_{\text{int}} = \mathcal{L}_{\text{int}}^{(1)} + \mathcal{L}_{\text{int}}^{(2)}$  captures spinon interactions,

$$\begin{aligned} \mathcal{L}_{\text{int}}^{(1)} &= u_1 \left( \sum_i \rho_i \right)^2 + u_2 \sum_{i \neq j} \rho_i \rho_j + u_3 \sum_{i \neq j} \vec{\mathcal{S}}_i \cdot \vec{\mathcal{S}}_j \\ &\quad + u_4 \sum_{[ijkl]} \phi_{i\alpha}^* \phi_{j\beta}^* \phi_{k\alpha} \phi_{l\beta} + u_5 \sum_{i \neq j} \phi_{i\alpha}^* \phi_{i\beta}^* \phi_{j\alpha} \phi_{j\beta} \\ \mathcal{L}_{\text{int}}^{(2)} &= w_1 \left( \sum_i \rho_i \right)^3 + w_2 \sum_{i,j,k} \epsilon^{ijk} \vec{\mathcal{S}}_i \cdot (\vec{\mathcal{S}}_j \times \vec{\mathcal{S}}_k) + \dots \end{aligned} \quad (6)$$

Latin indices label the 4 modes at  $\mathbf{Q}_i$  ( $i = 0, 1, 2, 3$ ), the notation  $[ijkl]$  implies all 4 modes are different, and there is an implicit sum on Greek indices which label spin or space-time. We defined  $\rho_i \equiv \phi_{i\alpha}^* \phi_{i\alpha}$  and  $\vec{\mathcal{S}}_i \equiv \phi_{i\alpha}^* \vec{\sigma}_{\alpha\beta} \phi_{i\beta}$ .  $\mathcal{L}_{\text{int}}^{(1)}$  and  $\mathcal{L}_{\text{int}}^{(2)}$  respectively list all quartic interactions and important sixth order terms, consistent with momentum conservation, global  $SU(2)$  symmetry, and local gauge invariance.  $u_{1,2}$  are forward-scattering interactions,  $u_{3,4}$  are backscattering terms, and  $u_5$  is an Umklapp process.  $w_2$  encodes broken time-reversal symmetry. At mean field level, with dominant  $u_1, w_1 > 0$ , we find  $r > 0$  leads to the CSL, while tuning  $r < 0$  leads to a confining Higgs phase with  $\langle \phi_{i\alpha} \rangle \neq 0$ . For  $u_2 < 0$ , we get simultaneous condensation at all  $\mathbf{Q}_i$ . The tetrahedral state emerges via a continuous transition for subdominant terms  $u_4, u_5 < u_3, w_2$  (see Supplemental Material [60]). Our construction of the field theory for the CSL-tetrahedral transition relies on a nontrivial flux pattern for the spinons, hinting at ‘crystal symmetry fractionalization’ [76] in the CSL.

**Summary.** Using ED and DMRG, we have shown that the Haldane-Hubbard Mott insulator supports unusual chiral magnetic orders, while third-neighbor hopping induces a CSL with topological order. We have argued that this CSL descends from a ‘parent’ tetrahedral state and constructed a CS-Higgs theory for this exotic spin-crystallization transition. Recent work has shown that the kagome lattice admits only a single  $SU(2)$  invariant symmetry enriched CSL [77, 78]. However, the honeycomb lattice may admit multiple CSLs with distinct crystal symmetry fractionalization patterns. Future research directions include nailing down the precise nature of this CSL [77–81], and relating this CSL to Gutzwiller projected wavefunctions [49, 50]. Another outstanding issue is fluctuation effects on the CS-Higgs transition proposed here, and in related  $U(1)$  symmetric bosonic quantum Hall to charge density-wave insulator transitions [82].

**Acknowledgments.** We thank R. Desbuquois, K. Hwang, G. Jotzu, S. Sachdev, and D.N. Sheng for useful discussions. CH and AP acknowledge support from NSERC of Canada. Computations were performed on the GPC supercomputer at the SciNet HPC Consortium. SciNet is funded by: the Canada Foundation for Innovation under the auspices of Compute Canada; the Government of Ontario; Ontario Research Fund - Research Excellence; and the University of Toronto. This work also made use of the facilities of N8 HPC Centre of Excellence, provided and funded by the N8 consortium and EP-SRC (Grant No.EP/K000225/1). The Centre is co-ordinated by the Universities of Leeds and Manchester. L.C. acknowledges support by the John Templeton Foundation. This research was supported in part by Perimeter Institute for Theoretical Physics. Research at Perimeter Institute is supported by the Government of Canada through Industry Canada and by the Province of Ontario through the Ministry of Research and Innovation.

- [1] M. König, S. Wiedmann, C. Brune, A. Roth, H. Buhmann, L. W. Molenkamp, X.-L. Qi, and S.-C. Zhang, *Science* **318**, 766 (2007).
- [2] D. Hsieh, D. Qian, L. Wray, Y. Xia, Y. S. Hor, R. J. Cava, and M. Z. Hasan, *Nature* **452**, 970 (2008).
- [3] L. X. Yang, Z. K. Liu, Y. Sun, H. Peng, H. F. Yang, T. Zhang, B. Zhou, Y. Zhang, Y. F. Guo, M. Rahn, D. Prabhakaran, Z. Hussain, S. K. Mo, C. Felser, B. Yan, and Y. L. Chen, *Nat Phys* **11**, 728 (2015).
- [4] B. Q. Lv, N. Xu, H. M. Weng, J. Z. Ma, P. Richard, X. C. Huang, L. X. Zhao, G. F. Chen, C. E. Matt, F. Bisti, V. N. Strocov, J. Mesot, Z. Fang, X. Dai, T. Qian, M. Shi, and H. Ding, *Nat Phys* **11**, 724 (2015).
- [5] S.-Y. Xu, N. Alidoust, I. Belopolski, Z. Yuan, G. Bian, T.-R. Chang, H. Zheng, V. N. Strocov, D. S. Sanchez, G. Chang, C. Zhang, D. Mou, Y. Wu, L. Huang, C.-C. Lee, S.-M. Huang, B. Wang, A. Bansil, H.-T. Jeng, T. Neupert, A. Kaminski, H. Lin, S. Jia, and M. Zahid Hasan, *Nat Phys* **11**, 748 (2015).
- [6] C.-Z. Chang, W. Zhao, D. Y. Kim, H. Zhang, B. A. Assaf, D. Heiman, S.-C. Zhang, C. Liu, M. H. W. Chan, and J. S. Moodera, *Nat Mater* **14**, 473 (2015).
- [7] A. J. Bestwick, E. J. Fox, X. Kou, L. Pan, K. L. Wang, and D. Goldhaber-Gordon, *Phys. Rev. Lett.* **114**, 187201 (2015).
- [8] L. Fidkowski and A. Kitaev, *Phys. Rev. B* **81**, 134509 (2010).
- [9] L. Fidkowski and A. Kitaev, *Phys. Rev. B* **83**, 075103 (2011).
- [10] X.-G. Wen, *Advances in Physics* **44**, 405 (1995).
- [11] S. A. Parameswaran, R. Roy, and S. L. Sondhi, *Comptes Rendus Physique* **14**, 816 (2013).
- [12] E. J. Bergholtz and Z. Liu, *International Journal of Modern Physics B* **27**, 1330017 (2013).
- [13] D. Pesin and L. Balents, *Nat Phys* **6**, 376 (2010).
- [14] S. Bhattacharjee, Y. B. Kim, S.-S. Lee, and D.-H. Lee, *Phys. Rev. B* **85**, 224428 (2012).
- [15] M. Kargarian, A. Langari, and G. A. Fiete, *Phys. Rev. B* **86**, 205124 (2012).
- [16] J. Maciejko, V. Chua, and G. A. Fiete, *Phys. Rev. Lett.* **112**, 016404 (2014).
- [17] F. D. M. Haldane, *Phys. Rev. Lett.* **61**, 2015 (1988).
- [18] G. Jotzu, M. Messer, R. Desbuquois, M. Lebrat, T. Uehlinger, D. Greif, and T. Esslinger, *Nature* **515**, 237 (2014).
- [19] M. Aidelsburger, M. Lohse, C. Schweizer, M. Atala, J. T. Barreiro, S. Nascimbene, N. R. Cooper, I. Bloch, and N. Goldman, *Nat Phys* **11**, 162 (2015).
- [20] P. W. Anderson, *Mater. Res. Bull.* **8**, 153 (1973).
- [21] V. Kalmeyer and R. B. Laughlin, *Phys. Rev. Lett.* **59**, 2095 (1987).
- [22] X. G. Wen, *International Journal of Modern Physics B* **04**, 239 (1990).
- [23] S. R. White, *Phys. Rev. Lett.* **69**, 2863 (1992).
- [24] I. P. McCulloch, [arXiv:0804.2509](https://arxiv.org/abs/0804.2509).
- [25] D. F. Schroeter, E. Kapit, R. Thomale, and M. Greiter, *Phys. Rev. Lett.* **99**, 097202 (2007).
- [26] R. Thomale, E. Kapit, D. F. Schroeter, and M. Greiter, *Phys. Rev. B* **80**, 104406 (2009).
- [27] Y.-C. He, D. N. Sheng, and Y. Chen, *Phys. Rev. Lett.* **112**, 137202 (2014).
- [28] B. Bauer, L. Cincio, B. P. Keller, M. Dolfi, G. Vidal, S. Trebst, and A. W. W. Ludwig, *Nat Commun* **5**, 5137 (2014).
- [29] S.-S. Gong, W. Zhu, and D. N. Sheng, *Scientific Reports* **4**, 6317 (2014).
- [30] K. Kumar, K. Sun, and E. Fradkin, *Phys. Rev. B* **90**, 174409 (2014).
- [31] S.-S. Gong, W. Zhu, L. Balents, and D. N. Sheng, *Phys. Rev. B* **91**, 075112 (2015).
- [32] A. Wietek, A. Sterdyniak, and A. M. Läuchli, [arXiv:1503.03389](https://arxiv.org/abs/1503.03389).
- [33] W. Zhu, S. S. Gong, and D. N. Sheng, [arXiv:1509.05509](https://arxiv.org/abs/1509.05509).
- [34] W.-J. Hu, W. Zhu, Y. Zhang, S. Gong, F. Becca, and D. N. Sheng, *Phys. Rev. B* **91**, 041124 (2015).
- [35] S. Bieri, L. Messio, B. Bernu, and C. Lhuillier, *Phys. Rev. B* **92**, 060407 (2015).
- [36] K. Kumar, K. Sun, and E. Fradkin, *Phys. Rev. B* **92**, 094433 (2015).
- [37] A. E. B. Nielsen, G. Sierra, and J. I. Cirac, *Nat Commun* **4** (2013).
- [38] D. Poilblanc, J. I. Cirac, and N. Schuch, *Phys. Rev. B* **91**, 224431 (2015).
- [39] M. Hermele, V. Gurarie, and A. M. Rey, *Phys. Rev. Lett.* **103**, 135301 (2009).
- [40] T. Meng, T. Neupert, M. Greiter, and R. Thomale, *Phys. Rev. B* **91**, 241106 (2015).
- [41] G. Gorohovsky, R. G. Pereira, and E. Sela, *Phys. Rev. B* **91**, 245139 (2015).
- [42] M. Oshikawa, *Phys. Rev. Lett.* **84**, 1535 (2000).
- [43] M. B. Hastings, *EPL (Europhysics Letters)* **70**, 824 (2005).
- [44] J. He, S.-P. Kou, Y. Liang, and S. Feng, *Phys. Rev. B* **83**, 205116 (2011).
- [45] J. He, Y.-H. Zong, S.-P. Kou, Y. Liang, and S. Feng, *Phys. Rev. B* **84**, 035127 (2011).
- [46] J. Maciejko and A. Rüegg, *Phys. Rev. B* **88**, 241101 (2013).
- [47] C. Hickey, P. Rath, and A. Paramekanti, *Phys. Rev. B* **91**, 134414 (2015).
- [48] W. Zheng, H. Shen, Z. Wang, and H. Zhai, *Phys. Rev. B* **91**, 161107 (2015).
- [49] Y. Zhang, T. Grover, and A. Vishwanath, *Phys. Rev. B* **84**, 075128 (2011).
- [50] Y. Zhang, T. Grover, A. Turner, M. Oshikawa, and A. Vishwanath, *Phys. Rev. B* **85**, 235151 (2012).
- [51] I. Martin and C. D. Batista, *Phys. Rev. Lett.* **101**, 156402 (2008).
- [52] K. Jiang, Y. Zhang, S. Zhou, and Z. Wang, *Phys. Rev. Lett.* **114**, 216402 (2015).
- [53] A. H. MacDonald, S. M. Girvin, and D. Yoshioka, *Phys. Rev. B* **37**, 9753 (1988).
- [54] A. Mulder, R. Ganesh, L. Capriotti, and A. Paramekanti, *Phys. Rev. B* **81**, 214419 (2010).
- [55] Fouet, J. B., Sindzingre, P., and Lhuillier, C., *Eur. Phys. J. B* **20**, 241 (2001).
- [56] A. F. Albuquerque, D. Schwandt, B. Hetényi, S. Capponi, M. Mambrini, and A. M. Läuchli, *Phys. Rev. B* **84**, 024406 (2011).
- [57] H. Mosadeq, F. Shahbazi, and S. A. Jafari, *Journal of Physics: Condensed Matter* **23**, 226006 (2011).
- [58] B. Bernu, C. Lhuillier, and L. Pierre, *Phys. Rev. Lett.* **69**, 2590 (1992).
- [59] B. Bernu, P. Lecheminant, C. Lhuillier, and L. Pierre, *Phys. Rev. B* **50**, 10048 (1994).
- [60] See Supplemental Material for more details on (i) the ED spectra for the magnetically ordered phases, (ii) fidelity cuts across the Néel-Tetrahedral phase boundary for  $N = 18, 24, 32$ , (iii) the comparison of the effective spin model phase diagram and spectra with only additional  $J_3$  terms versus further including all chiral terms generated by  $t_3$ , and (iv) the mean field treatment of the Chern-Simons Higgs theory.
- [61] P. Zanardi and N. Paunković, *Phys. Rev. E* **74**, 031123 (2006).

- [62] L. Messio, C. Lhuillier, and G. Misguich, *Phys. Rev. B* **83**, 184401 (2011).
- [63] H. Li and F. D. M. Haldane, *Phys. Rev. Lett.* **101**, 010504 (2008).
- [64] E. Rowell, R. Stong, and Z. Wang, *Commun. Math. Phys.* **292**, 343 (2009).
- [65] L. Cincio and G. Vidal, *Phys. Rev. Lett.* **110**, 067208 (2013).
- [66] M. P. Zaletel, R. S. K. Mong, and F. Pollmann, *Phys. Rev. Lett.* **110**, 236801 (2013).
- [67] W. Zhu, D. N. Sheng, and F. D. M. Haldane, *Phys. Rev. B* **88**, 035122 (2013).
- [68] A. Chandran, M. Hermanns, N. Regnault, and B. A. Bernevig, *Phys. Rev. B* **84**, 205136 (2011).
- [69] J. Dubail, N. Read, and E. H. Rezayi, *Phys. Rev. B* **86**, 245310 (2012).
- [70] B. Swingle and T. Senthil, *Phys. Rev. B* **86**, 045117 (2012).
- [71] X.-L. Qi, H. Katsura, and A. W. W. Ludwig, *Phys. Rev. Lett.* **108**, 196402 (2012).
- [72] X. G. Wen, *Phys. Rev. B* **41**, 12838 (1990).
- [73] P. Di Francesco, P. Mathieu, and D. Sénéchal, *Conformal field theory* (Springer, 1997).
- [74] Y. Zhang, T. Grover, A. Turner, M. Oshikawa, and A. Vishwanath, *Phys. Rev. B* **85**, 235151 (2012).
- [75] T. Senthil, A. Vishwanath, L. Balents, S. Sachdev, and M. P. A. Fisher, *Science* **303**, 1490 (2004).
- [76] A. M. Essin and M. Hermele, *Phys. Rev. B* **90**, 121102 (2014).
- [77] M. P. Zaletel, Z. Zhu, Y.-M. Lu, A. Vishwanath, and S. R. White, [arXiv:1511.01510](https://arxiv.org/abs/1511.01510).
- [78] L. Cincio and Y. Qi, [arXiv:1511.02226](https://arxiv.org/abs/1511.02226).
- [79] L. Wang, A. Essin, M. Hermele, and O. Motrunich, *Phys. Rev. B* **91**, 121103 (2015).
- [80] M. Zaletel, Y.-M. Lu, and A. Vishwanath, [arXiv:1501.01395](https://arxiv.org/abs/1501.01395).
- [81] Y. Qi and L. Fu, *Phys. Rev. B* **91**, 100401 (2015).
- [82] M. Barkeshli, N. Y. Yao, and C. R. Laumann, *Phys. Rev. Lett.* **115**, 026802 (2015).